

Contents lists available at ScienceDirect

Journal of Colloid and Interface Science

journal homepage: www.elsevier.com/locate/jcis



Regular Article

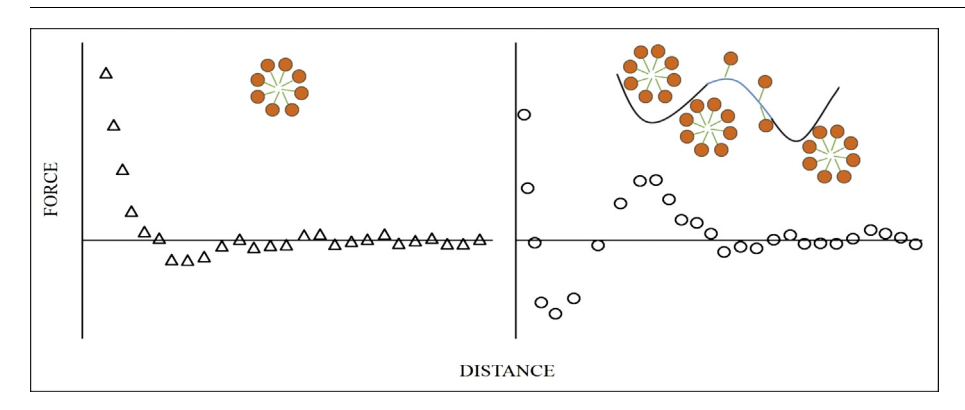
Control of the colloidal depletion force in nonionic polymer solutions by complexation with anionic surfactants



Bhagyashree J. Lele a, Robert D. Tilton a,b,*

- ^a Department of Chemical Engineering, Center for Complex Fluids Engineering, Carnegie Mellon University, 5000 Forbes Avenue, Pittsburgh, PA 15213, USA
- b Department of Biomedical Engineering, Center for Complex Fluids Engineering, Carnegie Mellon University, 5000 Forbes Avenue, Pittsburgh, PA 15213, USA

G R A P H I C A L A B S T R A C T



ARTICLE INFO

Article history:
Received 4 April 2019
Revised 7 June 2019
Accepted 9 June 2019
Available online 10 June 2019

Keywords:
Depletion forces
Structural forces
Polymer/surfactant complexes
Colloidal probe atomic force microscopy
Synergism

ABSTRACT

Hypothesis: Charge, size and concentration of depletants control the magnitude and range of depletion and structural forces. Noncovalent association of nonionic polymers with ionic surfactants may therefore synergistically enhance these forces to an extent that depends on the structure and composition of the resulting complexes.

Experiments: Forces were measured between a silica sphere and a silica plate in solutions of Pluronic F108 nonionic poly(ethylene oxide – block – propylene oxide – block – ethylene oxide) triblock copolymers and anionic sodium dodecylsulfate (SDS) surfactants using colloidal probe atomic force microscopy as a function of polymer, surfactant and NaCl background electrolyte concentrations. Trends in the magnitudes of the depletion attraction minimum and the first repulsive maximum in the oscillatory structural force were interpreted with the aid of pyrene solubilization assays, sodium ion-selective electrode analysis, and dynamic light scattering measurements that characterized the formation, charge, and hydrodynamic radius of F108/SDS complexes respectively.

Findings: Synergistic enhancement of the depletion force and first repulsive maximum occurred within a finite range of SDS concentrations, to an extent that depended on F108 and NaCl concentrations. This was due mainly to charging of F108/SDS complexes. Size effects were important at low NaCl concentration. Forces measured above the synergistic SDS concentration range were indistinguishable from those in polymer-free SDS solutions due to the appearance of excess unbound SDS micelles.

© 2019 Elsevier Inc. All rights reserved.

E-mail addresses: blele@andrew.cmu.edu (B.J. Lele), tilton@cmu.edu (R.D. Tilton).

^{*} Corresponding author at: Department of Chemical Engineering, Center for Complex Fluids Engineering, Carnegie Mellon University, 5000 Forbes Avenue, Pittsburgh, PA 15213, USA.

1. Introduction

In addition to the van der Waals and electrostatic double laver forces considered by the classical DLVO theory [1], a variety of other "non-DLVO" colloidal forces may act between surfaces in liquids. Depending on the system composition, these forces may include steric forces [2,3], bridging forces [4], or oscillatory structural forces [5-8], the first attractive minimum of which is known as the depletion force [9-13]. The structural forces are caused by non-adsorbed macromolecules, micelles, nanoparticles or similar nanoscale objects in the liquid phase and arise from packing constraints imposed on these objects in the narrow gap between surfaces. Thus, the force is primarily entropic in nature. The depletion force arises due to exclusion of those objects, often referred to as "depletants", from the gap upon sufficiently close approach of the two interacting surfaces. The resulting osmotic pressure difference between the bulk solution and the gap produces a stress that would drive the surfaces together: an apparent force of attraction that would act in addition to the van der Waals attraction and in opposition to any electrostatic or steric repulsion between the surfaces.

Inspection of the original Asakura and Oosawa [9,10] model of the depletion force provides useful insights into how the depletion force may respond to changes in solution conditions. The magnitude of the depletion interaction energy was assumed directly proportional to the osmotic pressure, Π , of the bulk solution. Factors that would increase the osmotic pressure of a depletant solution tend to increase the strength of the depletion attraction. This model, expressed here in terms of the interaction between a sphere of radius a and a flat plate as a function of surface-to-surface separation distance, h, gives the depletion interaction energy $\phi_{dep}(h)$ as [14]

$$\phi_{dep}(h) = -\pi \Pi a (2\Delta - h)^2 \qquad h < 2\Delta \tag{1}$$

$$\phi_{dep}(h) = 0 \qquad h > 2\Delta \tag{2}$$

The interaction exists for separation distances smaller than twice a depletion layer thickness, Δ , that equals the radius of the depletant, r_d , in the case of uncharged depletants. It is larger for charged depletants due to an electrostatic exclusion zone that scales with the Debye length, κ^{-1} , when the surfaces and depletants have the same sign of charge. Experimental observations [14] indicate that Δ is approximately $r_d+5\kappa^{-1}$ for hard spherical depletants. Thus, factors that increase (decrease) the size of the depletant, such as surfactant complexation with a polymer in a mixed solution, or factors that increase (decrease) the range of the electrostatic exclusion zone will contribute to an increase (decrease) in the strength of the depletion interaction.

Assuming ideality for simplicity, the osmotic pressure difference between the bulk and gap in solutions containing nonionic macromolecules with concentration, $\rho_{\infty m}$, is given by

$$\Pi = \mathsf{RT}\rho_{\infty m} \tag{3}$$

and for charged macromolecules with valence, |z|, and concentration, $\rho_{\infty m}$, in the absence of background electrolyte is given by [14]

$$\Pi = RT(|z|+1)\rho_{\infty m} \tag{4}$$

Thus charged polyelectrolytes tend to yield stronger depletion forces than uncharged depletants at similar concentrations, due to the contribution of counterions to the osmotic pressure [11,14–16]. Background electrolyte may affect the depletion force via several mechanisms, some of which tend to weaken the attraction [14], while others would strengthen it [17]. Among the major effects, first note that increasing electrolyte concentration decreases the Debye length and depletion layer thickness and

thereby decreases the range and magnitude of the depletion attraction imparted by charged depletants between charged surfaces (see Eqs. (1) and (2)). It also weakens the effect of polyelectrolytes in enhancing the osmotic pressure difference, which depends on background monovalent electrolyte concentration, ρ_{∞} , as [14]

$$\Pi = RT \left[(|z|+1)\rho_{\infty m} + 2\rho_{\infty s} \left(1 - \sqrt{\frac{|z|\rho_{\infty m}}{\rho_{\infty s}} + 1} \right) \right]$$
 (5)

The effect of polyelectrolyte on enhancing osmotic pressure difference relative to a nonionic polymer is eliminated at very high salt concentrations. For $\rho_{\infty s}$ >>|z| $\rho_{\infty m}$ the osmotic pressure reverts to

$$\Pi = \mathsf{RT}\rho_{\infty m} \tag{6}$$

When the depletants are ionic surfactant micelles, the increased screening of surfactant headgroup repulsions with increasing background electrolyte concentration decreases the critical micelle concentration (CMC) [17], thereby increasing the depletant concentration for any given concentration above the CMC and tending to enhance the magnitude of the depletion attraction.

When ionic surfactants complex with nonionic polymers, they impart charge to the polymer and introduce a polyelectrolyte character to their contribution to osmotic pressure and the depletion interaction. The onset of complexation at the critical association concentration (CAC) and the binding isotherm for ionic surfactant binding to polymers is sensitive to background electrolyte concentration. This introduces another manner in which electrolyte concentration may alter depletion forces in complexing systems.

The advent of sensitive force measurement techniques such as the surface force apparatus, total internal reflection microscopy and colloidal probe atomic force microscopy (CP-AFM) has enabled direct measurement of depletion and oscillatory structural forces. Depletion and oscillatory forces have been measured and predicted for various depletants including spherical nanoparticles [18], polymers [19], polyelectrolytes [20,21], micelles [22,23], non-spherical particles [24], and nanogels [25]. These measurements have focused primarily on systems containing a single type of depletant. Depletion forces between colloidal particles mediated by single component nanoscale depletants and their effects on colloidal phase behavior have been reviewed by Briscoe [26].

Motivated by the importance of multicomponent effects in commercially significant colloidal suspensions formulated with mixtures of surfactants and polymers, some studies have addressed depletion interactions in multicomponent systems. Supramolecular assemblies formed by polymer/surfactant complexation in solution and at interfaces have been thoroughly studied and reviewed [27–30]. Tulpar, Tilton and Walz [31] first observed synergistic enhancement of the depletion force due to polymer/surfactant complexation. That study reported the forces between a silica sphere and a flat silica plate in the presence of nonionic Pluronic F108 poly(ethylene oxide – block – propylene oxide - block - ethylene oxide) triblock copolymers and anionic sodium dodecylsulfate (SDS) surfactants. Ji and Walz [32] observed synergistic enhancement of depletion and structural forces caused by adsorption of poly(acrylic acid) polyelectrolytes (PAA) to solid nanoparticle depletants. In both cases, depletion force enhancement was due to complexation. Pluronic F108/SDS complexation endowed the polymer with a polyelectrolyte character whereby counterion osmotic pressure enhances the depletion force. Depletion force enhancement in the mixture of PAA and nanoparticles was attributed to the increased depletant size caused by PAA adsorption to the nanoparticles.

Our prior work on depletion forces in the Pluronic F108/SDS system [31] was limited to relatively low SDS concentrations and did not address the effects of background electrolyte. Here we consider a broader range of surfactant concentrations to address

changes that occur as the degree of complexation approaches and then exceeds saturation. We address a range of NaCl concentrations because this controls not only the complexation stoichiometry [17] but also the counterion contribution to the osmotic pressure of the "pseudo-polyelectrolyte" polymer/surfactant complex and the width of the electrostatic exclusion zone that extends the depletion layer thickness.

We use the CP-AFM method to measure structural and depletion forces between the negatively charged surfaces of a colloidal silica probe and a silica plate. We characterize the F108/SDS complexes using dynamic light scattering, sodium ion-selective electrode analysis and pyrene solubilization assays to investigate the parameters that control depletion forces in different concentration regimes, including the size, charge and binding regimes for F108/SDS complexation. We find that complexation synergistically enhances depletion forces at low SDS concentrations, and we identify a threshold SDS concentration above which depletion forces are indistinguishable from those in polymer-free SDS solutions due to the excess of free SDS micelles in solution. Finally we input measured characteristics of the F108/SDS complexes into the Walz and Sharma [33] depletion force model to compare experimental trends with theoretical expectations.

2. Experimental section

2.1. Materials

Pluronic F108, a nonionic triblock copolymer with the composition PEO₁₃₃-PPO₄₉-PEO₁₃₃ was provided by BASF Corp. Sodium dodecylsulfate (SDS) was purchased from Sigma-Aldrich (BioXtra grade, >99% purity) and was used as received. Purity was confirmed by the absence of a minimum in the surface tension isotherm near the CMC. All solutions containing SDS were prepared on the day of the experiment to minimize SDS hydrolysis to dodecanol. Water for all experiments was purified to 18.2 M Ω cm resistivity using a Thermo-Fisher Barnstead Nanopure Diamond system. Pyrene (\geq 99% GC) was purchased from Sigma-Aldrich. Sodium chloride, (Biotechnology grade) was purchased from VWR Life Science.

2.2. Methods

2.2.1. Colloidal probe atomic force microscopy

All forces were measured between a spherical silica probe particle and a flat silica plate using the CP-AFM technique [34] with a Bruker Multimode VIII AFM, operated in contact mode. Colloidal probes were prepared by attaching a 10 µm diameter silica sphere (Corpuscular Inc.) to the end of a tipless silicon nitride cantilever with reflective gold coating on the back side (Bruker MLCT-O10, B, nominal spring constant 0.02 N/m) using a UV-curable epoxy glue (Norland optical adhesive 63), which was cured using a UVozone ProCleaner (Bioforce Nanosciences) for 1 h after attachment. The spring constant for each cantilever was measured using the thermal tuning method [35]. The flat plates for force measurements were silica discs with a diameter of 12.7 mm, thickness of 3.18 mm and RMS roughness of 0.5 nm, purchased from CVI Laser Optics. These surfaces were cleaned prior to each experiment by soaking first in NOCHROMIX® (Godax Laboratories) mixed with sulfuric acid (MilliporeSigma) and then 6 N HCl (BDH Chemicals) for 20 min each and lastly in 10 mM NaOH (Fisher Scientific) for 30 min [36] with water rinses between each step. The AFM fluid cell (Bruker Model MTFML) was cleaned in purified water followed by 200 proof ethanol (Pharmco) and then dried using a nitrogen jet. Fluid cell tubing was sonicated in purified water prior to each experiment for 2 min and thoroughly rinsed to clean any adsorbed

polymers or surfactants that might remain from the previous experiment. Cleanliness was verified prior to each experiment by measuring the highly reproducible force between the bare silica probe and the bare disc in 0.1 mM NaCl solution prior to introducing the polymer and/or surfactant to solution.

After verifying surface cleanliness, approximately 10 times the liquid cell volume of the solution of interest was pumped through the liquid cell. After filling the cell, the system was allowed to equilibrate for 15 min before measuring forces. The sphere-to-plate approach and retract speeds were kept below 60 nm/s to decrease the hydrodynamic force on the cantilever to the point where it would not influence measured force curves [37]. Whereas force measurements made at velocities below 60 nm/s exhibited no detectable effect of speed, measurements made above 60 nm/s showed more repulsive approach and more attractive retract curves, indicating the influence of hydrodynamic forces [37]. For each solution composition, forces were measured at five different locations on the disc surface and an average force curve was calculated. This procedure was repeated in at least three independent experiments with freshly prepared solutions, discs and colloidal probes. All experiments were conducted in the temperature range of 22 ± 2 °C. After each experiment, the colloidal silica probe radius was determined by scanning electron microscopy (Hitachi 2460-N), and it was verified that the epoxy had not migrated along the probe to any location where it could interfere with the force measurement.

2.2.2. Pyrene solubilization

A pyrene solubilization assay [17,38] based on ultravioletvisible spectrophotometry was conducted to identify the CAC for the onset of SDS complexation with Pluronic F108 as well as transitions in the mode of binding and ultimately its saturation. Distinct binding regimes were identified by noting changes in pyrene solubilization power as a function of SDS concentration. For these measurements, an excess of pyrene powder was added to 10 mL sample solutions containing a fixed F108 concentration and spanning a range of SDS concentrations. Samples were bath sonicated for 8 h (Branson 1200 ultrasonic bath). Then, samples were equilibrated at room temperature (22 ± 2 °C) for an additional 12 h and centrifuged at 3000 rpm (1800 g) for 1 h (Eppendorf 5810 R) to remove any suspended solids. The absorbance of the supernatant was measured at 336 nm (Cary 300 UV-Vis spectrophotometer) and converted to pyrene concentration using its molar absorptivity $(2.06 \times 10^{-5} \text{ M cm})$ [17]. To ensure quantitative reliability of absorbance measurements, any sample for which the absorbance exceeded 1 was diluted by a standard solution of 130 mM SDS and 1000 ppm F108 for samples containing 1000 ppm F108 or 130 mM SDS and 10,000 ppm F108 for samples containing 10,000 ppm F108. This prevented precipitation of solubilized pyrene upon dilution.

2.2.3. Dynamic light scattering

Hydrodynamic radii of F108/SDS complexes formed in the presence of varying SDS concentrations were measured by dynamic light scattering using a Malvern Zeta Sizer Nano ZS at 173° backscatter angle. All samples were filtered for dynamic light scattering using 0.2 μ m polyethersulfone syringe filters. These measurements were conducted at 23° C.

Autocorrelation functions were fitted to determine distributions of translational diffusion coefficients using the CONTIN algorithm. As the F108/SDS complexes are highly charged, their diffusion coefficients are affected by long range electrostatic interactions among the complexes. It is therefore necessary to extrapolate diffusion coefficients to infinite dilution, in order to calculate the correct hydrodynamic radius via the Stokes-Einstein equation. This is non-trivial for polymer/surfactant complexes. We used the

infinite dilution diffusion coefficient analysis method that Brown and coworkers [39] developed for the PEO/SDS system. This method assumes that the size of polymer/SDS complexes is fixed for a fixed ratio of SDS to F108 concentration as long as the SDS concentration is above the CAC.

2.2.4. Sodium ion-selective electrode (ISE) analysis

The osmotic pressure, and thus the magnitude of the depletion force, depends on the number of charges per depletant, |z|. As sodium is the counterion for the F108/SDS complexes, a sodium ion selective electrode was used to determine |z| from the activity of free sodium ions in solution as a function of SDS concentration above the CAC, for a fixed F108 concentration in the presence of a constant 0.1 mM concentration of NaCl background electrolyte. Higher NaCl concentrations were not considered due to swamping of Na⁺ contributions from SDS at low surfactant concentrations. Measurements were made with an Orion Ross Combination Sodium Ion Selective Electrode and Orion Star A329 potentiometer. The electromotive force was converted to activity using the electrode constants obtained from calibration with NaCl solutions [40]. The sodium ion activity for F108/SDS mixtures was measured first at the highest SDS concentration, and then the sample was serially diluted with SDS-free F108 solution containing 0.1 mM NaCl. After each dilution, the next reading was taken after approximately 10 min to let the system equilibrate. During the measurement the sample was gently stirred until a stable reading was noted. All measurements were performed at 22 ± 2°C. This technique of measuring the counterion activity as a function of surfactant concentration was originally developed for anionic surfactant micellation [40,41]. We have extended it to polymer/surfactant complexation. It was determined in the micellization studies that counterions bound to micelles are not detected by the ionselective electrodes; only the free counterions contribute to the measured activity.

For SDS concentrations above the CAC but below the polymer/ surfactant binding saturation concentration, the measured Na⁺ activity in solution is divided among four sources of free Na⁺. Firstly, the background NaCl electrolyte contributes a constant concentration of free Na+. Secondly, since SDS is a strong electrolyte fully dissociated into Na⁺ and monovalent dodecylsulfate anions below the CAC, there is a constant free Na⁺ concentration that is equal to the CAC. Next, free Na⁺ corresponding to counterions dissociated from polymer-bound dodecylsulfate ions contribute to an extent that varies with the total SDS concentration. Finally, there is a free Na⁺ contribution corresponding to counterions of dodecylsulfate ions that are not bound to F108 and are therefore assumed to be in unimeric form and fully dissociated. This contribution to the measured Na⁺ activity also varies with total SDS concentration. The analysis here was restricted to SDS concentrations below the appearance of unbound SDS micelles in solution.

The determination of |z| requires a calculation of the fraction of the total number of sodium dodecylsulfate molecules beyond the CAC that are bound to F108. This is represented as θ . Similar to the definition of counterion binding fraction for surfactant micelles, the fraction of polymer-bound dodecylsulfate ions with bound Na⁺ counterions is represented as α . The concentration of sodium ions contributed from background electrolyte is constant and equal to C_{NaCl} ; from the completely dissociated SDS below CAC is constant and equal to CAC; from the unbound SDS molecules beyond CAC is $(1-\theta)\left(C_{SDS}^T-CAC\right)$; and from the dissociated counterions corresponding to polymer-bound dodecylsulfate ions is $(1-\alpha)\theta\left(C_{SDS}^T-CAC\right)$. These contributions together make up the total concentration of free sodium ions (C_{Na}) in the mixture:

$$C_{Na} = C_{NaCI} + CAC + (1 - \theta) \left(C_{SDS}^{T} - CAC \right) + (1 - \alpha) \theta \left(C_{SDS}^{T} - CAC \right)$$
(7)

Here, C_{SDS}^T refers to the total surfactant concentration added to the solution. The ion-selective electrode measures the activity of free Na⁺ ions (a_{Na}), which is related to C_{Na} by an activity coefficient, γ_{Na} , [40]:

$$a_{Na} = \gamma_{Na} C_{Na} \tag{8}$$

To determine, C_{Na} , from the measured activity, a_{Na} , the activity coefficient, γ_{Na} , is specified using the modified Debye-Hückel equation [42]

$$\gamma_{Na} = 10^{\left[\frac{Az^2\sqrt{I}}{1+a_{kejl}B\sqrt{I}}\right]} \tag{9}$$

where A and B are constants equal to $0.51 \,\mathrm{M}^{-0.5}$ and $3.32 \,\mathrm{nm}^{-1}$ - $\mathrm{M}^{-0.5}$, respectively, at room temperature, and the Kjelland parameter, a_{Kjel} , is $0.45 \,\mathrm{nm}$ for sodium ions [42]. The ionic strength, I, is calculated as:

$$I = \frac{z^{2}C_{Na} + z^{2}C_{CI} + z^{2}C_{DS}}{2}$$

$$= \frac{\left(2C_{NaCI} + 2CAC + (1 - \alpha)\theta\left(C_{SDS}^{T} - CAC\right) + 2(1 - \theta)\left(C_{SDS}^{T} - CAC\right)\right)}{2}$$
(10)

where z^2 is the square of valence of the ions contributing to the ionic strength and is equal to one here as sodium, chloride and dodecylsulfate ion are each univalent. Following Pashley and Ninham [43] for the lack of contribution of micelles to ionic strength, it was assumed that F108/SDS complexes likewise do not contribute to the ionic strength of the solution. The concentration of chloride ions, C_{Cl} , is equal to the background NaCl concentration, C_{NaCl} . The free dodecylsulfate ion concentration, C_{DS} , is

$$C_{DS} = CAC + (1 - \theta) \left(C_{SDS}^{T} - CAC \right)$$
(11)

The Na⁺ activity, a_{Na} , is measured as a function of the total SDS concentration, C_{SDS}^T . Eqs. (7)–(11) are combined to relate a_{Na} to C_{SDS}^T with α and θ as the unknowns. It is important to note that α and θ are not constants and indeed are functions of C_{SDS}^T . Models for α and θ are given below in Eqs. (12) and (13). The CAC value needed for the calculation is obtained from the pyrene solubilization assay.

In order to capture the essential idea that the number of dodecylsulfate ions bound per polymer must increase with increasing total SDS concentration and smoothly approach saturation, dodecylsulfate binding to F108 chains above the CAC was proposed to follow a Langmuir isotherm as the simplest model that would capture this behavior:

$$\frac{\theta(c_{SDS}^T - CAC)}{N_{max}} = \frac{N}{N_{max}} = \frac{(c_{SDS}^T - CAC)}{(c_{SDS}^T - CAC) + K}$$
(12)

In the above equation, N is the total concentration of polymerbound SDS and is equal to $\theta(c_{SDS}^T-\text{CAC})$. In this Langmuir model, N is normalized by N_{max} , the maximum concentration of SDS that can bind to F108 and K is the apparent equilibrium constant. Thus, N_{max} and K are fitting parameters.

It was further assumed that the fraction of Na $^+$ counterions dissociated from the polymer-bound dodecylsulfate ions, $(1-\alpha)$, decreases from unity at the CAC with increasing extent of dodecylsulfate binding to F108, since the increasing electrostatic repulsions among more closely packed dodecylsulfate ions would favor counterion binding. We thus formulated a Langmuirian model for the dependence of α on the total SDS concentration, as

a simple model that allows for a variable degree of counterion dissociation from polymer-bound dodecylsulfate ions:

$$(1-\alpha) = \frac{CAC}{\left(c_{SDS}^T - CAC\right)b + CAC} \tag{13}$$

where b is an empirical fitting parameter associated with the apparent counterion binding affinity for F108-bound dodecylsulfate ions. The equation follows the trend that the degree of counterion dissociation from polymer-bound dodecylsulfate ions decreases with increase in total SDS concentration as more and more SDS binds to F108 backbone. The concentration of undissociated sodium ions, i.e., the concentration of sodium ions bound to dodecylsulfate ions, at any given SDS concentration is αN .

Eqs. (7)–(13) describe the variation of free Na⁺ activity with respect to changing the total SDS concentration. This model was compared to measurements of Na⁺ activity vs c_{SDS}^T to fit for K, N_{max} and b using the Matlab optimization function *fmincon* (Matlab version R2016a, MathWorks). With these fitted parameters, we reconstruct the number of surfactants bound per polymer and the charge of the complexes |z| as functions of the total SDS concentration, as

$$|z| = \frac{(1 - \alpha) \left[\theta \left(c_{SDS}^T - CAC\right)\right]}{C_{F108}}$$
(14)

where C_{F108} is the F108 concentration. It is assumed that the concentration of F108/SDS complexes is the same as the F108 concentration.

3. Results and discussion

3.1. Force curve analysis: Effect of SDS and F108 concentrations

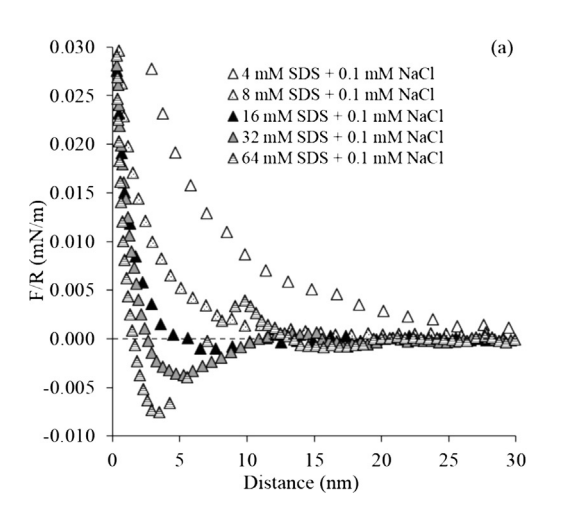
Representative force curves for a silica sphere interacting with a silica plate in NaCl solutions containing SDS alone or F108 alone are shown in Fig. 1. All forces were normalized by the measured radius of the spherical probe particle. Fig. 1a shows forces in SDS solutions ranging from 4 to 64 mM in the presence of 0.1 mM NaCl. Forces measured for 0 and 2 mM SDS are given in Supporting Material Fig. S1. Forces were purely repulsive for SDS concentrations of 0, 2, 4 and 8 mM and were consistent with exponentially decaying electrostatic double layer forces, as expected for non-micellar solutions. The exponential decay lengths for these conditions were 33.0, 6.3, 4.9, and 3.5 nm respectively, consistent with the Debye lengths that correspond to those ionic strengths based

on fully dissociated SDS plus 0.1 mM NaCl concentrations (30.3, 6.6, 4.7, and 3.4 nm respectively).

Evidence of a depletion attraction was observed for 16 mM SDS as a minimum in the force curve at approximately 7.5 nm apparent surface separation distance. Increasing the SDS concentration to 32 and then to 64 mM deepened the attractive well, shifted the force minimum to smaller separation distances, and produced a prominent repulsive barrier at 9 nm for 64 mM SDS. The attraction at small separation distance and repulsion at large distance is characteristic of the oscillatory structural forces previously observed in micellar surfactant solutions [22,23]. The inward shift of the force minimum is due to the increase in the strength of the depletion attraction superimposed on the electrostatic double layer repulsion between the surfaces. It should be noted that anionic SDS does not adsorb to negatively charged silica surfaces [17,44,45].

Force curves were measured for 1.000 and 10.000 ppm F108 solutions that contained no SDS. F108 micelles were not expected at either of these concentrations, as the CMC of F108 at 22 °C is approximately 70,000 ppm [46]. Fig. 1b shows that forces in these F108 solutions were purely repulsive, even at a background NaCl concentration of 100 mM, which was intentionally made large to fully screen double layer repulsions and reveal any indication of a depletion force. No evidence for a depletion attraction was observed. The repulsion was of a significantly longer range than would be expected for the double layer force, and the force curves were not smoothly decaying, indicating steric repulsion between adsorbed F108 layers. This is consistent with prior observations of F108 adsorption to silica [17]. At 0.1 mM NaCl, the force profiles with either 1,000 or 10,000 ppm F108 were purely repulsive and exhibited a smooth exponential decay that was indistinguishable from the long range electrostatic double layer force with 0.1 mM ionic strength (See Supporting Material Fig. S2). The threshold cantilever deflection was set relatively low in those measurements to avoid damaging the probe, and thus the forces were measured with minimal overlap of adsorbed F108 layers and minimal influence of steric forces at the smaller separation distances.

Forces were measured at twelve different SDS concentrations in the presence or absence of F108, for a constant 0.1 mM NaCl concentration. Fig. 2 depicts the force profiles in SDS-only and F108/SDS mixed solutions for selected SDS concentrations ranging from 4 to 64 mM. These conditions capture the trends observed upon addition of 1,000 or 10,000 ppm F108 to a solution of SDS. All force measurements conducted for SDS concentrations below 128 mM were non-hysteretic: forces measured on approach were indistinguishable from forces measured on separation of the surfaces. In



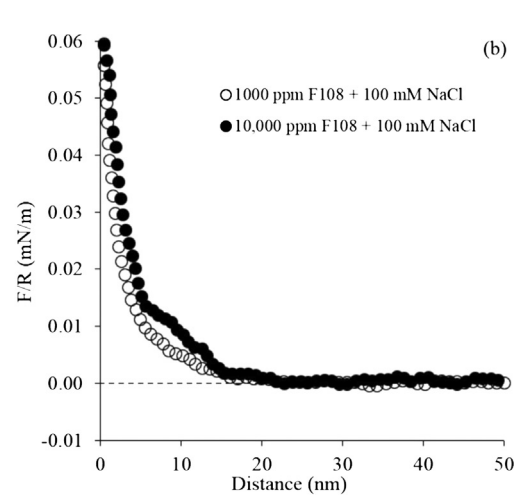


Fig. 1. Normalized approach force profiles between silica sphere and fused silica disc in solution containing (a) SDS alone in the presence of 0.1 mM NaCl or (b) F108 alone in the presence of 100 mM NaCl background electrolyte.

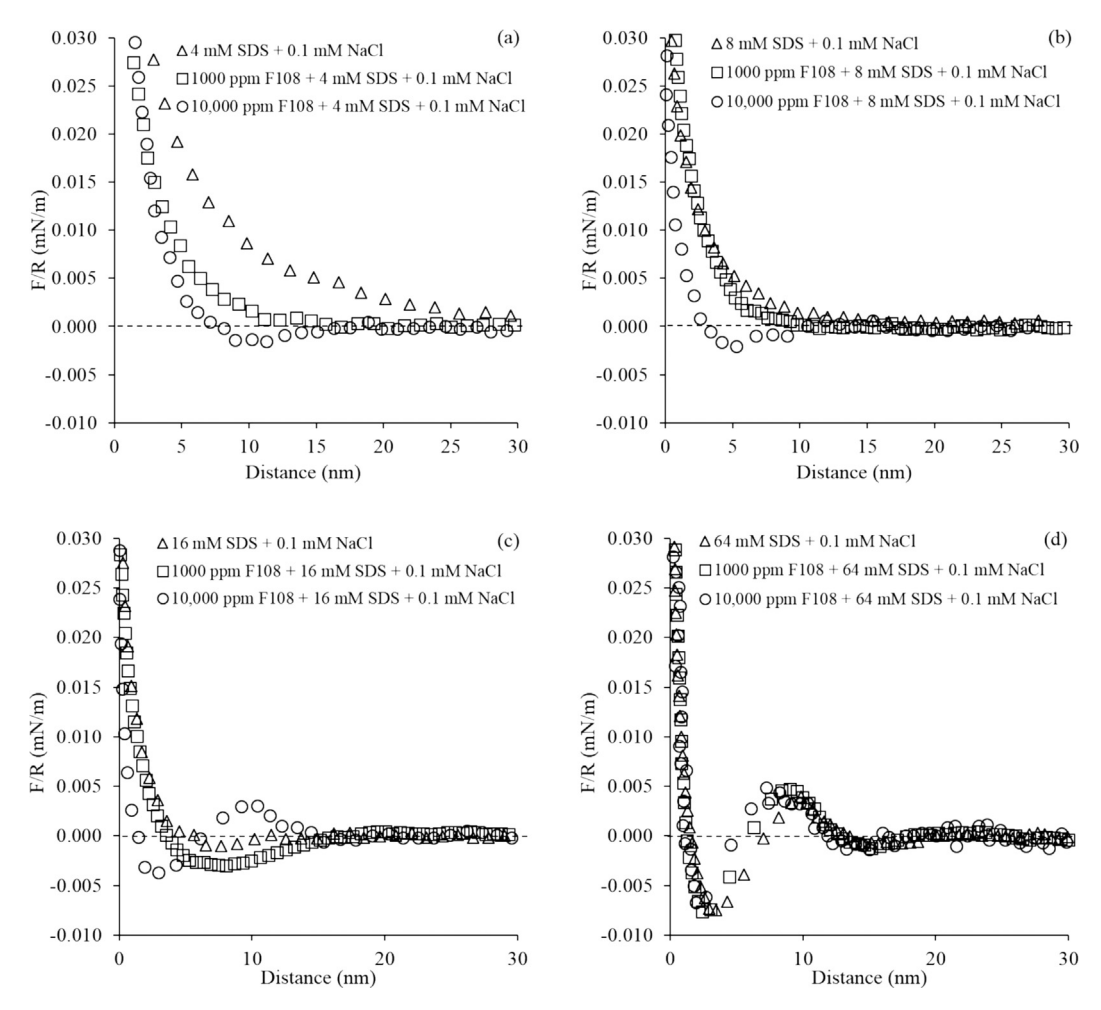


Fig. 2. Representative normalized force profiles for selected SDS concentrations with 0, 1000 or 10,000 ppm F108. (a) 4 mM SDS (b) 8 mM SDS (c) 16 mM SDS (d) 64 mM SDS. Background electrolyte concentration was 0.1 mM NaCl.

solutions containing 128 mM SDS with or without F108, the strong depletion attraction caused a jump into surface contact at the point where the force gradient exceeded the cantilever spring constant. Hence, we did not analyze the forces at or beyond 128 mM SDS concentration.

In the presence of 4 mM SDS (Fig. 2a), while the force remained purely repulsive for 1,000 ppm F108, an attractive minimum occurred with 10,000 ppm F108. Although no attractive minimum occurred in the mixture of 4 mM SDS and 1,000 ppm F108, the repulsive force was of significantly shorter range than the electrostatic double layer repulsion in the solution of 4 mM SDS alone. This indicates that a depletion attraction was contributing to the net interaction between the surfaces. With 8 mM SDS (Fig. 2b), addition of 10,000 ppm F108 again produced an attractive force minimum. The forces in the 1,000 ppm F108 still produced no minimum, and now deviated only slightly from the double layer repulsion in the 8 mM SDS solution (which has a smaller Debve length than the solution of 4 mM SDS). With 16 mM SDS (Fig. 2c), all three mixtures exhibit rather distinct force profiles. All exhibit depletion attraction minima, but the minima are significantly deeper with 1,000 and 10,000 ppm F108 than with 16 mM SDS alone, and the 10,000 ppm F108 solution now exhibits a pronounced repulsive maximum associated with the oscillatory structural force. Finally, with 64 mM SDS, all three mixtures exhibited both an attractive depletion force minimum and a repulsive structural force maximum. The depth of the minima and the height of the maxima were similar for all three solutions.

The force profile results for selected SDS concentrations in Fig. 2 revealed synergistic depletion force and structural force enhancement. The onset of a primary minimum in the net force profile was observed at significantly lower SDS concentrations when F108 was present. In the presence of 1,000 or 10,000 ppm F108, attractive minima were first observed with 10 mM or 4 mM SDS, respectively, whereas an attractive minimum was first observed at 16 mM SDS in the absence of F108. Thus, the presence of F108 introduced a strong depletion attraction at concentrations below the CMC of SDS. The occurrence of a depletion attraction in F108/ SDS mixtures at SDS concentrations where no attraction was observed for solutions of either SDS or F108 alone is attributed to the binding of dodecylsulfate anions to uncharged F108. This forms a charged F108/SDS complex that is larger than a F108 chain in SDS-free solution, effectively creating a pseudo-polyelectrolyte. Details of the charge and size of F108/SDS complexes will be presented below. Inspection of Eqs. (1)–(6) shows that increasing size and charge of the depletant both strengthen the depletion attraction, consistent with this observation of synergistic enhancement of the depletion attraction.

In order to summarize the dependence of the depletion force strength on the SDS and F108 concentrations, the depth of the attractive force minimum was extracted from each force curve and plotted as a function of SDS concentration in Fig. 3a. A synergistic enhancement of the depletion attraction was most clearly observed at low SDS concentrations (see inset), where neither SDS alone nor F108 alone produced depletion attractions. Synergis-

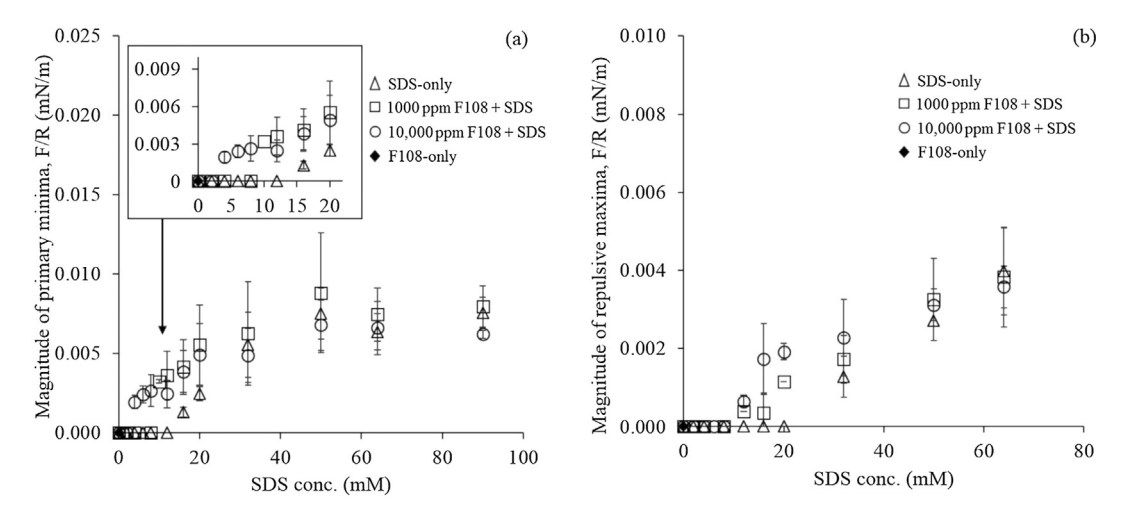


Fig. 3. Summary plots for the magnitude of (a) the primary minimum or (b) the repulsive maximum in the net force profiles as a function of SDS concentration with and without polymer. Background electrolyte concentration was 0.1 mM NaCl.

tic enhancement only occurred in a finite range of SDS concentrations corresponding to approximately 4 to 20 mM SDS for solutions containing 10,000 ppm F108 and 10 to 20 mM SDS concentration for solutions containing 1,000 ppm F108. At SDS concentrations of ~ 30 mM and above, the magnitude of the force minimum was indistinguishable for mixtures or solutions of SDS alone. We propose that at these higher SDS concentrations, both charged F108/SDS complexes and free SDS micelles contribute to the depletion attraction, and the relative contribution of the complexes becomes small as the free SDS micelles become increasingly abundant. Important transitions in the mode of binding and the relative abundance of free micelles and complexes will be discussed in the section below.

It is important to note that although it is plausible that the aggregation number or degree of ionization of SDS micelles could change under confinement in the gap between the silica surfaces relative to the bulk, SDS micelles in bulk solution remain spherical over the full range of SDS and background NaCl concentrations investigated here [47,48]. Thus, any changes in forces associated with increasing SDS concentration cannot be attributed to changes in the structure of free micelles. Another important issue to note is that in the lower range of SDS concentrations, there is likely an additional electrosteric repulsion force that would oppose the depletion force, due to adsorption of F108/SDS complexes [17]. Using ellipsometry, we confirmed that F108/SDS complexes adsorb on silica surfaces at lower SDS concentrations (Supporting Material Section III). Adsorption was not observed beyond 16 mM SDS concentration for either F108 concentration, consistent with results reported previously [17]. It was not possible to discern an electrosteric force from the measured force profiles, but the effect of such an additional repulsion would be to partly mask the depletion attraction.

Just as complexation enhanced the depletion attraction, it enhanced the repulsive barrier associated with the oscillatory structural force as shown in Fig. 3b. These barriers are evident at higher SDS concentrations and they become increasingly prominent as the SDS concentration increases. In the absence of F108, this repulsive barrier was observed in the net force profile for SDS concentrations of 32 mM and above. In the presence of 1,000 or 10,000 ppm F108, a repulsive barrier was observed for SDS concentrations of 12 mM and above. The magnitude of the repulsive barrier was greater for 10,000 ppm F108 than for 1,000 ppm. This shows that the creation of highly charged and larger complexes affected the way in which these depletants organize in the gap between two surfaces at larger separations. This strengthened

the consequent repulsive structural force compared to free SDS micelles. Similar to the synergistic enhancement of the depletion attraction, the synergistic enhancement of the repulsive barrier was observed in a finite SDS concentration range. Repulsive barrier heights for mixtures and SDS-only solutions became indistinguishable for measurements made at 50 mM SDS and above.

3.2. Force curve analysis: Effect of background electrolyte concentration

Since the background electrolyte concentration affects not only the thermodynamics of F108/SDS binding, but also the osmotic pressure and the range of the electrostatic exclusion zone, it is expected to significantly influence depletion interactions. Thus, forces were compared for solutions containing F108 with varying SDS concentrations for either 0.1, 10 or 100 mM NaCl. Results are summarized in Fig. 4.

In these experiments, the F108 concentration was fixed at 10,000 ppm and SDS concentrations were varied between 0 and 90 mM. Increasing the background electrolyte concentration affected the magnitude of the depletion force as well as the SDS concentration range over which synergistic enhancement was observed in mixtures. Comparing representative force profiles for 32 mM SDS solutions in the presence of 10,000 ppm F108 and varying NaCl concentrations (Fig. 4a) shows that increasing NaCl concentration decreased the magnitude of both the attractive minimum and the repulsive barrier. At 100 mM NaCl, neither an attractive minimum nor a repulsive maximum were discernable in the mixture of 10,000 ppm F108 with 32 mM SDS.

Examining the summary of the magnitudes of the attractive minima for varying SDS concentrations in Fig. 4b shows that increasing NaCl concentration weakened the depletion attraction for any given SDS concentration with or without polymer. Increasing NaCl concentration also increased the minimum SDS concentration at which a primary attractive minimum was first detected, either with or without the presence of polymer. For example, for mixtures in the presence of 100 mM NaCl, in SDS-only solutions the primary minimum was not detected at all, whereas for 0.1 mM and 10 mM NaCl, the primary minimum was first observed at 16 and 32 mM SDS respectively. This reflects both the reduction in osmotic pressure (see Eq. (5)) and the reduction in depletion layer thickness (see Eq. (1)).

Despite the effect of increasing background electrolyte to dampen depletion forces, an enhancement in the depth of the primary attractive minimum in the presence of 10,000 ppm F108 was still

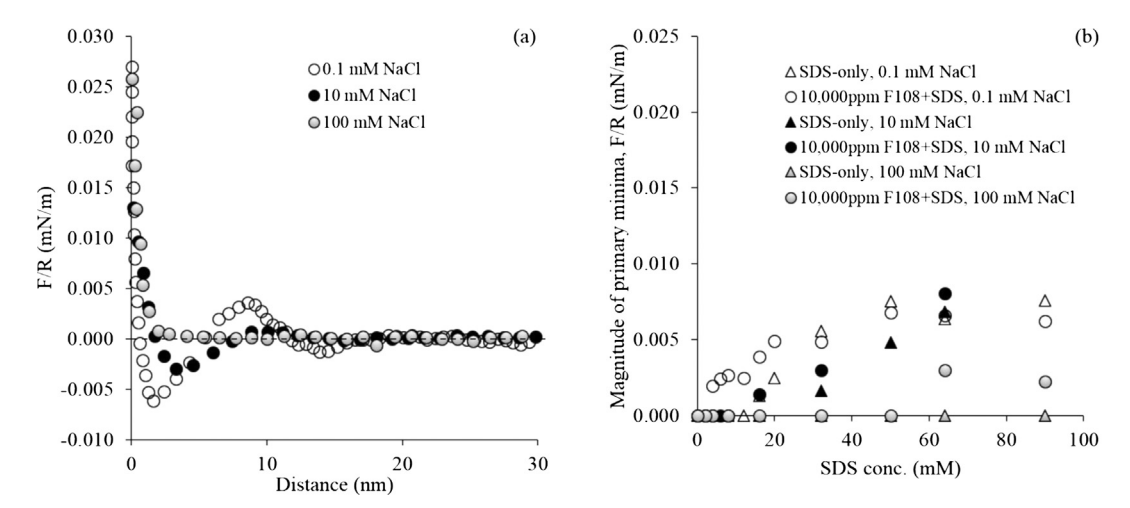


Fig. 4. (a) Representative force profiles for 32 mM SDS in the presence of 10,000 ppm F108 at 0.1, 10 or 100 mM NaCl as background electrolyte. (b) Summary plot of the magnitudes of primary attractive minima from the net force profiles for 0.1, 10 or 100 mM NaCl for solutions.

observed, relative to SDS alone, in the presence of 10 and 100 mM NaCl (Fig. 4b). Although significantly higher SDS concentrations were required to observe the depletion attraction in 100 mM NaCl (above 50 mM SDS) relative to the lower NaCl concentrations, the presence of the polymer did indeed enhance depletion attractions in the presence of this high background electrolyte concentration. This shows that even at high salt concentration binding of SDS to F108 leads to formation of a pseudo-polyelectrolyte complex with greater potency for inducing depletion attractions. F108 by itself did not produce any depletion attraction or repulsive structural force at any of these NaCl concentrations. At 100 mM NaCl, the repulsive barrier was not observed for 10,000 ppm F108 for any SDS concentration under investigation. For 10 mM NaCl, a repulsive barrier was observed only in the solutions containing 64 mM and 90 mM SDS, and the magnitudes of these barriers were about four times lower than in the 0.1 mM NaCl solutions for the same SDS concentrations.

Enhancement of the depletion attraction was produced by addition of 10,000 ppm F108, relative to the attraction produced in the corresponding polymer-free SDS solution, even at the highest NaCl concentration (100 mM) under investigation, where the osmotic pressure enhancement due to counterions is weakened but not eliminated. While complexation did still enhance depletion attractions in the presence of 0.1, 10 and 100 mM NaCl, the overall effect

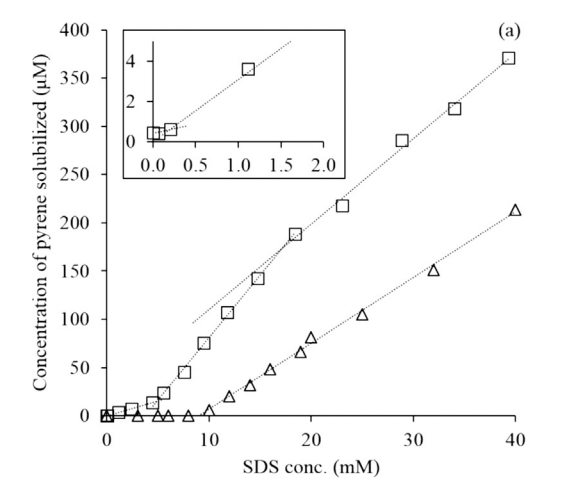
of increasing background electrolyte concentration is to weaken the attraction. The result is forces that are generally more repulsive for a given separation distance in SDS solutions or F108/SDS mixed solutions that contain more NaCl, despite the greater screening of the electrostatic double layer force in the more concentrated NaCl solutions.

3.3. Characterization of F108/SDS complexes

To better understand the observed synergistic enhancement of the depletion attraction that was caused by F108 addition to SDS solutions, including the fact that the enhancement only occurred within a finite range of SDS concentrations, we investigated the modes of binding, the size of complexes and the charge of complexes formed in different SDS concentration ranges. This information was obtained from pyrene solubilization, dynamic light scattering and sodium ion activity measurements.

3.3.1. Pyrene solubilization

Comparing pyrene solubilization in SDS solutions in the presence or absence of F108 reveals transitions in the mode of SDS self-assembly from the formation of F108-bound complexes to the formation of free micelles. Fig. 5 shows the dependence of the concentration of pyrene solubilized as a function of SDS con-



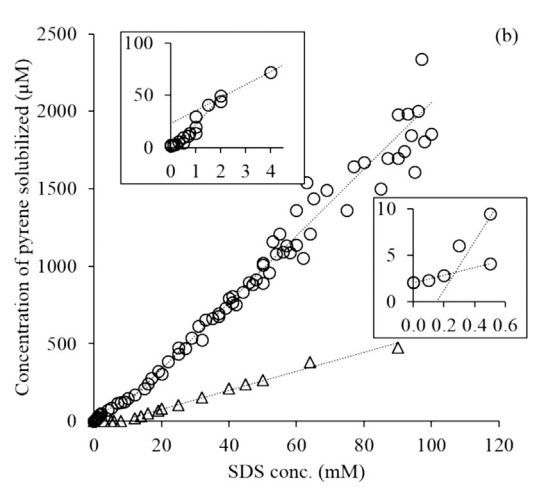


Fig. 5. Pyrene solubilization assays for F108/SDS solutions containing (a) 1,000 ppm F108 or (b) 10,000 ppm F108. Background electrolyte concentration was 0.1 mM NaCl. Unfilled triangles represent SDS with no F108 (same data reproduced for comparison in both panels). Squares and circles represent 1,000 and 10,000 ppm F108 solutions respectively.

centration for both F108 concentrations under investigation. Different modes of SDS self-assembly produce different slopes, i.e. different solubilizing powers [38].

For the case of 1,000 ppm F108, the pyrene solubilization assay shows four well-defined regimes with easily discernable slopes, culminating in apparent saturation near 17 mM SDS. The slope in the pyrene solubilization plot for 1,000 ppm F108 beyond 17 mM SDS concentration is similar to that of SDS-only solutions beyond the CMC (8.9 mM), indicating the prevalence of free SDS micelles as more SDS is added to solution beyond 17 mM SDS concentration. Different solubilizing powers likely reflect different molecular arrangements on the F108 chain as discussed previously [17]. The first distinct change of slope occurs at 0.2 mM SDS concentration as shown by the inset in Fig. 5a. This marks the onset of binding and hence the CAC of SDS. Below 0.2 mM SDS concentration the slope is almost zero indicating the absence of SDS assemblies.

For any SDS concentration, the concentration of pyrene solubilized was significantly greater for 10,000 ppm F108 than for 1,000 ppm F108. This may be due at least in part to pyrene solubilization by association with the hydrophobic poly(propylene oxide) block [49], and it is simply more pronounced in the more concentrated F108 solution. Direct solubilization by F108 was evident in the non-zero intercept for solubilized pyrene concentration at zero SDS concentration. These solutions are still well below the CMC of F108, so solubilization in polymer micelles is not a factor. The inset of Fig. 5b indicates that the CAC remains approximately 0.2 mM for 10,000 ppm F108, based on a distinct slope change at that concentration. In the range of SDS concentrations examined, no concentration regime was identified where the solubilizing power in the mixture was similar to the solution of SDS alone. It is probable that the saturation concentration had not yet been reached, or that both free micelles and complexes were forming simultaneously at the high end of the considered SDS concentration range for 10,000 ppm F108. Pyrene solubilization results obtained here for 0.1 mM NaCl are consistent with previously reported results for 1,000 ppm F108 solutions [17]. The prior study established that increasing NaCl concentration to 10 and then to 150 mM slightly decreased the CAC and had little effect on the binding saturation concentration.

Pyrene solubilization gave evidence for F108/SDS binding saturation at 17 mM in the case of 1,000 ppm F108. In the context of the depletion force measurements, this means that any new depletants formed by SDS self-assembly at higher concentrations would be free micelles, and as the SDS concentration was further increased, the free micelles would become the predominant depletants. This is the likely explanation for the loss of synergistic enhancement of the depletion force beyond 20 mM SDS concentration. For 10,000 ppm F108 solutions, no evidence for binding saturation was obtained for SDS concentrations as large as 90 mM, yet the loss of synergistic depletion force enhancement for this higher F108 concentration was still observed beyond 20 mM SDS. During binding at the high polymer concentration, SDS molecules must be distributed over a larger number of chains, and we hypothesize that surfactants may form free micelles in parallel with their binding to F108 chains. This has been noted in prior studies of SDS binding to nonionic polymers [50]. Those free micelles could again become the majority depletants and lead to the loss of synergistic enhancement of the depletion force at high SDS concentrations in the presence of 10,000 ppm F108.

3.3.2. Dynamic light scattering

Since the depletion interaction is sensitive to the size of the depletant, dynamic light scattering was used to determine the hydrodynamic diameters of the species present in solution for varying SDS and F108 concentrations. The sensitivity of the hydro-

dynamic diameter to the relative concentrations of SDS and F108 also provides insight into the mode of SDS self-assembly that complements the pyrene solubilization assay. The charge and size of the SDS/F108 complexes are not constant but depend on the SDS concentration. To obtain the hydrodynamic diameter of a polyelectrolyte or other highly charged species in solution, one would perform DLS measurements for serial dilutions and extrapolate to infinite dilution to account for the effect of long-range interactions on the diffusion coefficient.

Brown and coworkers [39] developed a method to acquire the infinite dilution diffusion coefficient, and thus the true hydrodynamic diameter, for PEO/SDS complexes as a function of SDS concentration. We used this method here, which is applicable for surfactant concentrations between the CAC and the binding saturation concentration. Thus, dilutions were conducted for a fixed SDS/F108 concentration ratio to maintain a constant number of surfactants bound per polymer while decreasing the overall concentration of complexes. The diffusion coefficient, D, of charged species varies with the species concentration as $D = D_0(1 + k_D C)$, where C is the species concentration (polymer/surfactant complexes in this case), D_0 is the diffusion coefficient at infinite dilution, and k_D is the concentration coefficient proportional to the second virial coefficient.

Diffusion coefficients were obtained from the peak of the intensity-weighted distribution determined by the CONTIN algorithm. Monomodal diffusion coefficient distributions for a SDS/F108 mass ratio of 3.7 with varying F108 concentration are shown in Supporting Material Section IV to illustrate representative trends. Fig. 6a shows representative examples of the dependence of the diffusion coefficient on the concentration of F108 for three values of the fixed SDS/F108 mass ratio. Ten such ratios were tested to obtain infinite dilution diffusion coefficients for different SDS/F108 ratios, and thus for different extents of binding. For each SDS/F108 ratio, F108 concentrations where the diffusion coefficients no longer varied linearly with increasing F108 concentration were not analyzed. Hence 10,000 ppm F108 could not be considered in this analysis since the apparent diffusion coefficient no longer varied linearly with F108 concentration.

Diffusion coefficients were fitted to a line and extrapolated to zero concentration. The resulting infinite dilution diffusion coefficients are plotted against SDS/F108 mass ratio in Fig. 6b. As the SDS/F108 ratio increased from zero to 3.7, D_o initially decreased, corresponding to an increase in hydrodynamic diameter of the complexes with increasing amounts of SDS binding to F108. The associated increase in negative charge would tend to swell the complexes. Beyond a ratio of 3.7, D_o increased. This is attributed to a weakened swelling effect because of the increased screening provided by dissociated sodium counterions coming from the free SDS micelles, as explained by Brown and coworkers for SDS/PEO complexation [39]. The minimum in D_o at the ratio of 3.7 marked the saturation of polymer/surfactant binding.

Fig. 6c shows that k_D increases as a function of SDS/F108 ratio until 4.2. This demonstrates the increasing importance of longrange electrostatic repulsions among the complexes as they acquire increasing charge with increasing SDS binding. Beyond a ratio of 4.2, k_D decreases as the repulsive contribution is increasingly screened by the dissociated sodium counterions noted above. The maximum in k_D is also an indication of binding saturation of F108. This maximum occurred at a ratio of 4.2, close to the 3.7 ratio for the minimum in D_0 .

The hydrodynamic diameters corresponding to these SDS/F108 ratios, calculated via the Stokes-Einstein equation using infinite dilution diffusion coefficients, are plotted in Fig. 6d. The independent variable shown on the abscissa is the SDS concentration corresponding to each SDS/F108 ratio if the F108 concentration were

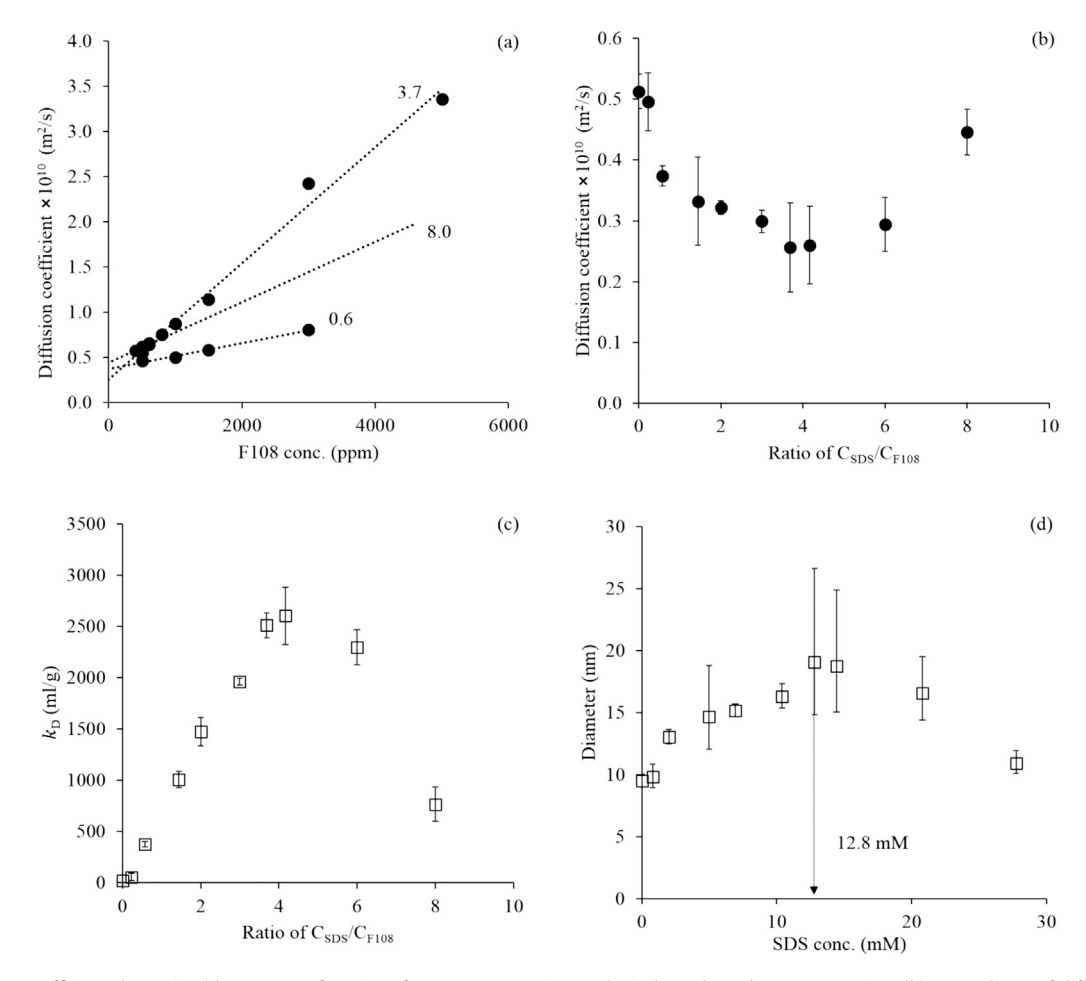


Fig. 6. (a) Diffusion coefficient determined by DLS as a function of F108 concentration at the indicated C_{SDS}/C_{F108} mass ratios. (b) Dependence of diffusion coefficient at infinite dilution on the C_{SDS}/C_{F108} mass ratio. (c) Concentration coefficient based on intermolecular repulsive interactions as a function of C_{SDS}/C_{F108} mass ratio. (d) Hydrodynamic diameter of F108/SDS complexes with increasing SDS concentration for 1,000 ppm F108. The arrow indicates a maximum diameter at 12.8 mM SDS. Background electrolyte concentration was 0.1 mM NaCl.

1,000 ppm. First note that the hydrodynamic diameter of F108 in the absence of SDS is 9.5 ± 0.5 nm, consistent with the size of a non-micellized F108 chain in aqueous solution reported elsewhere [31]. The diffusion coefficient for nonionic F108 in the absence of SDS was a weak function of F108 concentration in the range considered, due to the lack of long-range electrostatic repulsions (Supporting Material Section V).

The location of the maximum in hydrodynamic diameter in Fig. 6d indicates that the saturation of F108/SDS binding occurred at approximately 13 mM SDS for 1,000 ppm F108. Complexation with SDS produced a significant growth in hydrodynamic diameter to a maximum of \sim 19 nm, nearly a two-fold increase from the diameter of an F108 chain in solution. The swelling observed in the PEO/SDS system by Brown and coworkers [39] increased the hydrodynamic diameter at the point of saturation by a factor of approximately 1.6 relative to SDS-free PEO. That study was based on PEO with a molecular weight of 996,000.

The conclusion from dynamic light scattering and pyrene solubilization assay is that complexation in the 1,000 ppm F108 solutions has saturated at SDS concentrations below 20 mM SDS, where force measurements indicated the loss of synergistic depletion force enhancement. Furthermore, the size distributions obtained from dynamic light scattering for 1,000 ppm F108 at SDS concentrations of 20 mM and above exhibited distinct peaks arising from complexes and from free micelles (See Supporting Material Section IV). This supports the interpretation that the loss

of synergistic depletion force enhancement was due to the emergence of free SDS micelles as the majority depletants at high concentrations. Thus, concentrated SDS solutions with or without F108 produced similar depletion forces. Both DLS and pyrene solubilization data indicate that the predominant depletant in solutions containing 1,000 ppm F108 and 0.1 mM NaCl would be SDS/F108 complexes for SDS concentrations up to approximately 13 to 17 mM, and free micelles would dominate at higher concentrations.

The hydrodynamic diameter analysis that showed an increase in the size of the F108/SDS complexes until saturation is also consistent with the argument that one of the reasons for the observed synergistic enhancement of depletion forces is the increase in depletant size, as expected from Eqs. (1) and (2). As 10,000 ppm F108 solutions could not be included in the DLS study for reasons explained above, we were unable to determine the infinite dilution hydrodynamic diameter of the F108/SDS complexes with 10,000 ppm F108.

The infinite dilution DLS analysis for F108/SDS complexes was performed for 10 and 100 mM NaCl, and the results are reported in Supporting Material Section VI. For these higher NaCl concentrations, the hydrodynamic diameter of the F108/SDS complexes displayed a maximum at 2 mM SDS for both NaCl concentrations but then returned to a size similar to the unbound F108 chains at higher SDS concentrations. The diminished swelling of complexes at the higher NaCl concentrations relative to the strong swelling

at 0.1 mM NaCl is attributed to the enhanced screening of the charges imparted by polymer-bound dodecylsulfate ions. The screening effect of NaCl addition also decreased k_D relative to 0.1 mM NaCl solutions, but this concentration coefficient continued to increase with increasing SDS/F108 mass rations, even with 100 mM NaCl. This confirms the formation of charged complexes at all NaCl concentrations considered. The decreased swelling of charged complexes and the weakening of electrostatic repulsions arising from the complexes are responsible for the smaller magnitudes of depletion forces measured in F108/SDS solutions at higher NaCl concentrations (Fig. 4a).

The final result of the DLS analysis addresses a concern that high NaCl concentrations may alter the assembly and phase behavior of F108 in solution. Prior studies have indicated that certain salts at high concentrations affect the hydration and hence the phase separation temperatures of Pluronic polymers and PPO homopolymer chains [51,52]. DLS results obtained in the absence of SDS confirmed that the infinite dilution diffusion coefficient, and hence the hydrodynamic diameter of the F108 chains, was independent of NaCl concentration under the conditions of this study. Thus, no NaCl-induced F108 self-assembly or phase separation occurred in these systems.

3.3.3. Sodium ion selective electrode measurements

Self-assembly of SDS, whether in the form of free micelles or polymer-bound aggregates, decreases the activity of Na⁺ counterions depending on the extent of counterion binding to the assemblies. Sodium ion activity data from ISE measurements for various SDS and F108 concentrations in the presence of a constant 0.1 mM NaCl background electrolyte are shown in Fig. 7a. ISE measurements were only made for 0.1 mM NaCl background electrolyte concentration. The abscissa of the plot is NaCl concentration only for the NaCl reference line measured in the absence of SDS or F108. For all other conditions, the abscissa is SDS concentration.

The effect of counterion binding to micelles is evident in the data for SDS in the absence of F108, where Na⁺ activity increases approximately linearly with increasing SDS concentration until the slope decreases abruptly at 7.2 mM. The slope change is due to counterion binding to SDS micelles and indicates a CMC of \sim 7.2 mM. This is lower than the CMC inferred from pyrene solubilization (8.9 mM), since sodium ion activity would be affected by any pre-micellation assembly that may occur but which might not produce aggregates capable of solubilizing detectable amounts of pyrene. The ratio of the slopes immediately above and below the CMC is a good indication of the degree of counterion binding to micelles. This data indicate approximately 77% counterion binding to SDS micelles, which matches very well with the literature values [53,54]. Below the CMC, the Na⁺ ion activity increase with increasing SDS is indistinguishable from the Na⁺ activity measured in reference solutions of increasing NaCl concentration, as expected for complete dissociation of non-micellar SDS. We have confirmed that the presence of F108 does not affect the measurement of the free sodium ion activity using sodium ISE (See Supporting Material Section VII).

Since the decrease in Na⁺ activity relative to a fully dissociated state is to due to Na⁺ counterion association with dodecylsulfate assemblies, information about the number of dodecylsulfate surfactants bound per polymer and the fraction of those bound surfactants that have an associated Na⁺ counterion can be extracted by applying the activity model expressed as Eqs. (7)–(13) to the ISE data in Fig. 7a. It should be noted that the measured sodium ion activity is quite similar for both the F108 concentrations in the SDS concentration range under investigation. The CAC could not be detected from the ISE data: there was no abrupt change in the

shape of the curve at low SDS concentrations. As discussed below, this lack of an abrupt change is attributed to the nearly complete counterion dissociation of polymer-bound SDS molecules at concentrations near the 0.2 mM CAC that was revealed by the pyrene solubilization assay. The ISE cannot distinguish between the sodium ions coming from unbound dissociated SDS and those from polymer-bound dissociated SDS. Therefore the decrease in Na⁺ activity relative to the fully dissociated state only becomes apparent when the degree of counterion dissociation of the bound SDS deviates from unity.

The model was fitted to the experimental data for 1,000 and 10,000 ppm F108 concentrations. The analysis was conducted for SDS concentrations up to 15 mM, near the binding saturation concentrations determined for 1,000 ppm F108 via pyrene solubilization and DLS measurements. This was done because the current model does not include free micelles formed at higher SDS concentrations. The model was fitted to the experimental data to obtain the fitting parameters by minimizing the squared error. Fig. 7a shows that the model fits the experimental data well for both F108 concentrations. Values obtained for the empirical fitting parameters $N_{\rm max},~K$ and b are $1.8\pm0.8~M,~2.4\pm1.1~M$ and $0.047\pm0.005~$ for 1,000~ ppm F108 and $0.14\pm0.008~M,~0.18\pm0.015~M$ and $0.08\pm0.008~$ for 10,000 ppm F108 respectively. Information extracted from the model fitting is summarized in Fig. 7b–d and in Fig. 8.

Error bars on the parameters and calculated points in Fig. 7b–d and Fig. 8 were obtained by fitting the activity model for two independent ISE data sets. It should be noted that the fitted values of N_{max} and K were found to be proportional to each other; their ratio remained essentially constant at about 0.75 when fitting the data sets for 1,000 and 10,000 ppm F108. This coupling is responsible for the large uncertainty in the individual values of N_{max} and K. This is a characteristic of fitting Langmuir isotherm constants when the available data are for concentrations well below the isotherm plateau (see Eqs. (12) and (13)), in which case the ratio of N_{max}/K is the significant parameter.

The Na⁺ activity dependence on SDS concentration for 1,000 ppm F108 was guite similar to 10,000 ppm F108 in the SDS concentration range measured (0 to 15 mM). This suggests little quantitative effect of F108 concentration on the thermodynamics of complexation and counterion binding. Using Eqs. (12) and (13) and the fitted model parameters, we plotted in Fig. 7b and c the fraction of sodium dodecylsulfate molecules in the system that were bound to F108 chains, θ, and the degree of Na⁺ dissociation from polymer-bound dodecylsulfate ions, 1- α , as a function of total SDS concentration. Fig. 7b indicates that θ was nearly constant at \sim 0.75 over the range of 0.2–15 mM SDS and was rather similar for both polymer concentrations. The 10,000 ppm F108 data showed a mild decrease in θ with increasing SDS concentration. Thus, not every surfactant added to solution between the CAC and the saturation concentration joins a complex; they distribute between polymer-bound and unbound states in solution, as noted in other SDS/nonionic polymer binding systems [50]. Accordingly, the concentration of unbound SDS molecules in solution, $(1 - \theta)(C_{SDS}^T - CAC) + CAC$, grows nearly linearly with increasing total SDS concentration for both 1,000 and 10,000 ppm F108 solutions. This is plotted in Fig. 7d. The unbound SDS concentrations in solution at a total SDS concentration of 15 mM were calculated to be 3.8 and 4.7 mM, for 1,000 and 10,000 ppm F108, respectively. These are both below the SDS CMC, supporting the assertion made above that complexes, rather than free micelles, are the predominant depletants below $\sim 20 \text{ mM}$ SDS.

The degrees of counterion dissociation $(1 - \alpha)$ plotted in Fig. 7c are fairly similar for 1,000 and 10,000 ppm F108 at each SDS con-

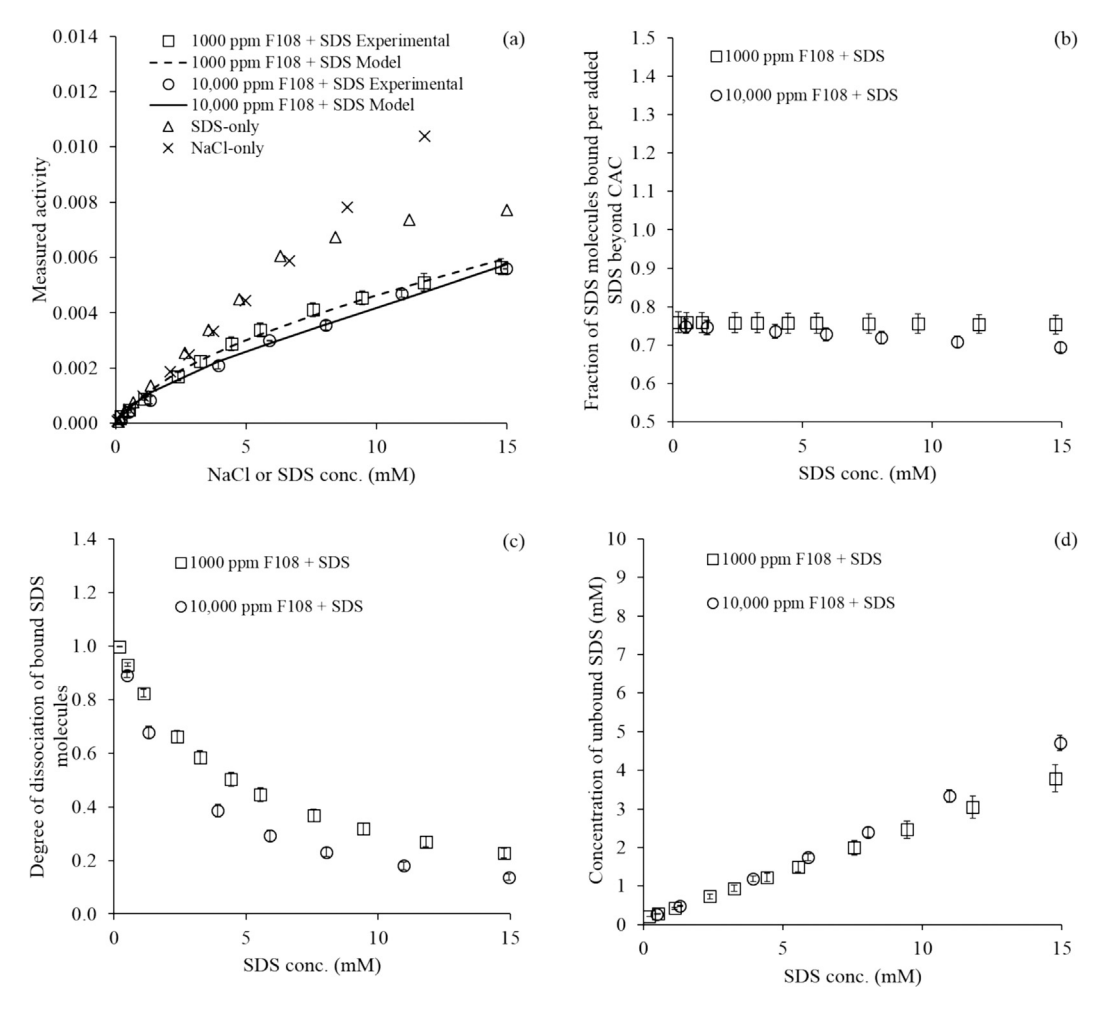


Fig. 7. (a) Experimental Na* activity ISE data for varying SDS concentrations in the presence of 0.1 mM NaCl with either 0, 1,000 or 10,000 ppm F108, or for reference NaCl solutions containing various NaCl concentrations but no SDS or F108. Curves show model fits for SDS/F108 mixtures. (b) Fraction of SDS molecules binding to F108, θ, as a function of total added SDS concentration, C_{SDS}^T , beyond CAC. (c) Fraction of counterions dissociated from polymer-bound SDS molecules, $1 - \alpha$, as a function of total SDS concentration, C_{SDS}^T . (d) Concentration of unbound SDS molecules in solution, CAC $+ (1 - \theta)C_{SDS}^T$, as a function of total SDS concentration, C_{SDS}^T . Background electrolyte is 0.1 mM NaCl.

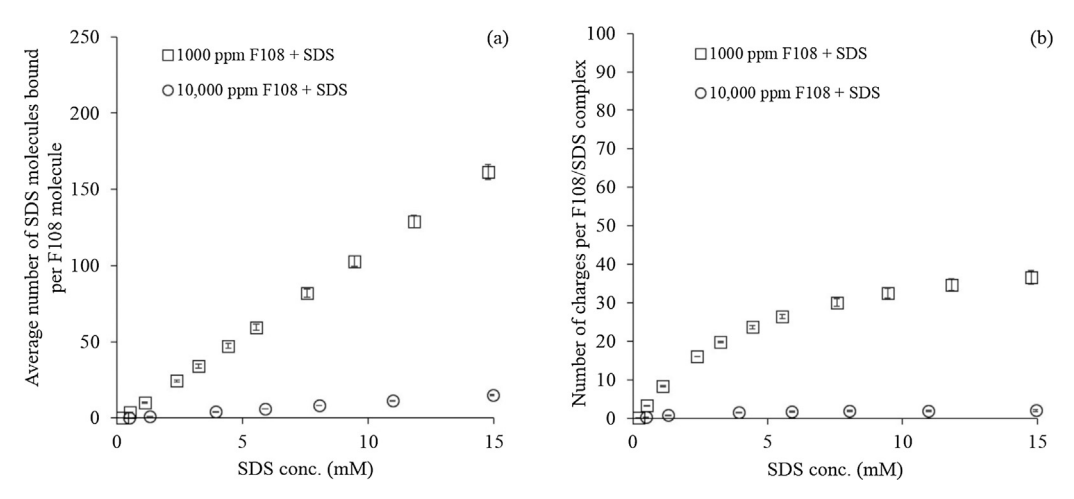


Fig. 8. (a) Number of SDS molecules bound per F108 molecule as a function of total SDS concentration, $\theta\left(C_{SDS}^T - CAC\right)/C_{F108}$ vs C_{SDS}^T . (b) Number of charges per complex |z|, corresponding to the number of dissociated sodium ions per complex as a function of total SDS concentration, $(1 - \alpha)\theta\left(C_{SDS}^T - CAC\right)/C_{F108}$ vs C_{SDS}^T . Background electrolyte is 0.1 mM NaCl.

centration, despite the ten-fold difference in F108 concentration. At the onset of binding, the degree of dissociation was assumed to be unity in the model, consistent with the lack of an abrupt

change in free Na⁺ activity at the onset of binding in Fig. 7a. As the SDS concentration increased the value of counterion dissociation decreased smoothly to 0.23 and to 0.14 for 1,000 and

10,000 ppm F108, respectively. These values are similar to the observed degree of dissociation of free SDS micelles, 0.23, measured in the absence of F108. This suggests that polymer-bound dodecylsulfate aggregates exhibit molecular packing that is comparable to that in free micelles, since head group proximity plays an important role in the thermodynamics of counterion binding. In the case of PEO homopolymer binding, the arrangement of SDS micelle-like clusters in a string of pearls configuration has been demonstrated experimentally [55–58]. Although surfactants may arrange themselves differently along the PPO and PEO blocks of F108, the ISE data suggest that on average, they exhibit micelle-like counterion binding and thus micelle-like cooperative assembly.

Although further research would be needed on this matter, the implication of similar cooperativity in binding with a ten-fold difference in polymer concentration could further imply polydispersity in the amount of surfactant bound to discrete polymer chains. It is known that polydispersity in the charge of depletants can dampen the depletion force [59]. It is possible, though our data cannot prove or disprove, that charge polydispersity might be dampening the depletion force in solutions containing SDS and 10,000 ppm F108.

Finally, to estimate the average charge of the complexes, the concentration of polymer-bound dodecylsulfate anions was assumed to be equally distributed among all of the polymer chains. Thus the average number of sodium dodecylsulfate molecules per chain is N/C_{F108} . This is plotted as a function the total SDS concentration in Fig. 8a, and the average number of charges per complex, |z|, was calculated according to Eq. (14) and plotted in Fig. 8b. The assumption of uniform distribution of charge among all polymer chains produces approximately ten-fold more dodecylsulfates bound per chain and ten-fold greater charge per complex for 1,000 ppm than for 10,000 ppm F108. While the possibility of polydispersity in binding is not addressed by this data, this average behavior is the result of the similarity of the measured changes in Na⁺ activity for 1,000 and 10,000 ppm F108. Hence, it is clear from the ISE data that the charge per F108/SDS complex increases as more SDS binds to the polymer with an increase in bulk SDS concentration. This is true for both the F108 concentrations under

As a check on assumptions made in the ISE model, we independently determined |z| for F108/SDS complexes at two different SDS concentrations in solutions containing 1000 ppm F108 and 0.1 mM NaCl by performing dialysis experiments with a titrating surfactant ion selective electrode (Supporting Material Section VIII). Results from the dialysis method matched those obtained by the sodium ion selective electrode measurements.

3.4. Theoretical examination of the consistency of force profiles with measured properties of complexes.

The depletion force depends on the size, charge and concentration of depletants; the Debye length consistent with the ion concentrations in the solution; and the charge of the surfaces bathed by the solution. To probe the consistency of measured changes in depletion forces with the properties of the complexes determined here in the presence of 0.1 mM NaCl, we fed the hydrodynamic diameters obtained from dynamic light scattering and the average charge per complex from the ISE analysis, as well as the concentrations of unbound dodecylsulfate ions and free sodium ions in solution calculated from the ISE data, into the Walz and Sharma depletion force model [33]. Full details of the model and its implementation here are presented in Supporting Material Section IX.

Theoretical force profiles were generated for 1,000 ppm F108 and SDS samples with 0.1 mM NaCl background electrolyte concentration. We could not obtain theoretical force profiles for

10,000 ppm F108 and SDS samples due to lack of hydrodynamic diameter measurements from infinite dilution diffusion coefficient analysis. We observed that the model consistently over-predicted the magnitude of the depletion forces in solutions both with and without the polymer, by a factor of approximately 4–9. Reasons for the quantitative over-prediction based on model assumptions are discussed in the Supporting Material. Most importantly, the synergistic enhancement of the depletion force in F108/SDS mixtures relative to the depletion force in polymer-free SDS solutions was observed to be same for the experimental and theoretical results. This supports the interpretation of depletion force enhancement as the result of an increased size of complexes and the pseudo-polyelectrolyte effect of imparting charge by anionic surfactant binding to the nonionic polymer.

4. Conclusions

Colloidal probe AFM measurements of the force between a silica sphere and silica plate confirmed a previously observed [31] synergistic enhancement of the attractive depletion force and the repulsive barrier associated with the oscillatory structural force in solutions containing anionic sodium dodecylsulfate surfactants and nonionic Pluronic F108 polymers. By examining the effects of surfactant, polymer and electrolyte concentration, and probing the physical characteristics of the complexes, this work determined the bounds of synergism and the coupled factors that control these forces in different solution composition regimes.

Synergism was found to exist within a finite range of SDS concentrations. The onset of synergism occurred well below the normal SDS critical micelle concentration and occurred at a lower SDS concentration when the F108 concentration was higher. Within the finite synergistic concentration range, both the depletion attraction and the repulsive barrier were greater in magnitude for the higher F108 concentration at a given SDS concentration. The upper end of the synergistic concentration range was the same for both polymer concentrations, corresponding to approximately twice the normal SDS CMC. Increasing the concentration of NaCl background electrolyte between 0.1 and 100 mM weakened the magnitudes of both the depletion attraction and the repulsive structural force barrier, but these forces in SDS/F108 mixtures were consistently enhanced relative to polymer-free SDS solutions for each of these background electrolyte concentrations. Complementary probes of surfactant/polymer complexation showed that its effects on the size and charge of the dominant depletant species dictate the magnitude of synergistic force enhancement and the surfactant concentration range over which synergism occurs. In the presence of dilute background electrolyte, both charging and swelling of complexes contribute to the depletion and structural force synergism. At higher background electrolyte concentrations, swelling plays a diminished role in the synergistic enhancement.

Depletion and oscillatory structural forces in systems containing a single type of depletant species are well understood [5,9,12,15,23,33]. This work enhances the fundamental understanding of depletion and structural colloidal forces in multicomponent systems containing polymers and surfactants that self-assemble into mixed complexes that may become the dominant depletant. Such systems are common in complex fluid products. The propensity to synergistic effects is a critical attribute of such systems and should be considered in their formulation. In synergistic systems, colloidal forces, and thus colloidal suspension phase behavior and rheology, cannot be predicted on the basis of the forces imparted by any individual component acting in isolation. It may be expected that major trends in these systems will be well represented by the current SDS/F108 system. In contrast to relatively simple single-component systems, changing the concentra-

tion of one or both components of these significantly more complex mixed systems not only changes the depletant concentration but may also change the depletant size and charge and may even shift the identity of the dominant depletant, for example from mixed complexes to free micelles, all in an ionic strength-dependent manner.

This work considered amphiphilic polymers that are capable of micellization, albeit at concentrations that are well below the polymer CMC and at temperatures that are well below a critical micelle temperature. There is evidence that surfactant binding can profoundly affect polymer micellization, especially if the temperature is close to the critical micelle temperature [60–63]. Future work may address the alteration of polymer micellization by surfactant binding in different concentration regimes and the corresponding effects on the associated depletion and structural forces.

Funding

This material is based on work supported by the National Science Foundation under grant CBET-1608003.

Acknowledgment

The authors thank Joseph Suhan for help with SEM measurements and John Walz and Shunxi Ji for providing their depletion force model code

Appendix A. Supplementary material

Supplementary data to this article can be found online at https://doi.org/10.1016/j.jcis.2019.06.026.

References

- [1] J. Israelachvili, Intermolecular and surface forces, Elsevier (2011), https://doi. org/10.1016/C2009-0-21560-1.
- [2] W. Liang, T.F. Tadros, P.F. Luckham, Flocculation of sterically stabilized polystyrene latex particles by adsorbing and nonadsorbing poly(acrylic acid), Langmuir. 10 (1994) 441–446, https://doi.org/10.1021/la00014a018.
- [3] D. Napper, Steric stabilization, J. Coll. Interf. Sci. 58 (1977) 390–407, https://doi.org/10.1016/0021-9797(77)90150-3.
- [4] C. Lu, R. Pelton, PEO flocculation of polystyrene-core poly(vinylphenol)-shell latex: an example of ideal bridging, Langmuir 17 (2001) 7770–7776, https://doi.org/10.1021/la0108930.
- [5] S. Biggs, R.R. Dagastine, D.C. Prieve, Oscillatory packing and depletion of polyelectrolyte molecules at an oxide-water interface, J. Phys. Chem. B. 106 (2002) 11557–11564, https://doi.org/10.1021/jp026425k.
- [6] O. Théodoly, J.S. Tan, R. Ober, C.E. Williams, V. Bergeron, Oscillatory forces from polyelectrolyte solutions confined in thin liquid films, Langmuir. 17 (2001) 4910–4918, https://doi.org/10.1021/la001820s.
- [7] M.L. Fielden, R.A. Hayes, J. Ralston, Oscillatory and ion-correlation forces observed in direct force measurements between silica surfaces in concentrated CaCl₂ solutions, Phys. Chem. Chem. Phys. 2 (2000) 2623–2628, https://doi.org/ 10.1039/b0016721.
- [8] N.C. Christov, K.D. Danov, Y. Zeng, P.A. Kralchevsky, R. Von Klitzing, Oscillatory structural forces due to nonionic surfactant micelles: data by colloidal-probe AFM vs theory, Langmuir. 26 (2010) 915–923, https://doi.org/10.1021/ la902397w.
- [9] S. Asakura, F. Oosawa, Interaction between particles suspended in solutions of macromolecules, J. Polym. Sci. 33 (1958) 183–192, https://doi.org/10.1002/ pol.1958.1203312618.
- [10] S. Asakura, F. Oosawa, On Interaction between two bodies immersed in a solution of macromolecules, J. Chem. Phys. 22 (1954) 1255–1256, https://doi. org/10.1063/1.1740347.
- [11] A.J. Milling, B. Vincent, Depletion forces between silica surfaces in solutions of poly(acrylic acid), J. Chem. Soc. Faraday Trans. 93 (1997) 3179–3183, https:// doi.org/10.1039/a701795b.
- [12] M. Piech, J.Y. Walz, Depletion interactions produced by nonadsorbing charged and uncharged spheroids, J. Coll. Interf. Sci. 232 (2000) 86–101, https://doi. org/10.1006/jcis.2000.7194.
- [13] P.A. Kralchevsky, K.D. Danov, S.E. Anachkov, Depletion forces in thin liquid films due to nonionic and ionic surfactant micelles, Curr. Opin. Coll. Interf. Sci. 20 (2015) 11–18, https://doi.org/10.1016/j.cocis.2014.11.010.

- [14] P.C. Odiachi, D.C. Prieve, Effect of added salt on the depletion attraction caused by non-adsorbing clay particles, Coll. Surf. A Physicochem. Eng. Asp. 146 (1999) 315–328, https://doi.org/10.1016/S0927-7757(98)00781-X.
- [15] E.S. Pagac, R.D. Tilton, D.C. Prieve, Depletion attraction caused by unadsorbed polyelectrolytes, Langmuir 14 (1998) 5106–5112, https://doi.org/10.1021/ la980058f.
- [16] S. Biggs, D.C. Prieve, R.R. Dagastine, Direct comparison of atomic force microscopic and total internal reflection microscopic measurements in the presence of nonadsorbing polyelectrolytes, Langmuir 21 (2005) 5421–5428, https://doi.org/10.1021/la050041e.
- [17] A.D. Braem, D.C. Prieve, R.D. Tilton, Electrostatically tunable coadsorption of sodium dodecyl sulfate and poly(ethylene oxide)- b -poly(propylene oxide)- b -poly(ethylene oxide) triblock copolymer to silica, Langmuir 17 (2001) 883– 890, https://doi.org/10.1021/la0013042.
- [18] D. Herman, J.Y. Walz, Adsorption and stabilizing effects of highly-charged latex nanoparticles in dispersions of weakly-charged silica colloids, J. Coll. Interf. Sci. 449 (2015) 143–151, https://doi.org/10.1016/j.jcis.2014.11.022.
- [19] D. Rudhardt, C. Bechinger, P. Leiderer, Direct measurement of depletion potentials in mixtures of colloids and nonionic polymers, Phys. Rev. Lett. 81 (1998) 1330–1333, https://doi.org/10.1103/PhysRevLett. 81.1330.
- [20] A. Sharma, S.N. Tan, J.Y. Walz, Effect of nonadsorbing polyelectrolytes on colloidal interactions in aqueous mixtures, J. Coll. Interf. Sci. 191 (1997) 236– 246, https://doi.org/10.1006/jcis.1997.4940.
- [21] S. Ji, J.Y. Walz, Depletion flocculation induced by synergistic effects of nanoparticles and polymers, J. Phys. Chem. B. 117 (2013) 16602–16609, https://doi.org/10.1021/jp410159a.
- [22] G.K. James, J.Y. Walz, Experimental and theoretical investigation of the depletion and structural forces produced by ionic micelles, Coll. Surf. A Physicochem. Eng. Asp. 441 (2014) 406–419, https://doi.org/10.1016/ i.colsurfa.2013.09.033.
- [23] G.K. James, J.Y. Walz, Experimental investigation of the effects of ionic micelles on colloidal stability, J. Coll. Interf. Sci. 418 (2014) 283–291, https://doi.org/ 10.1016/j.jcis.2013.12.015.
- [24] C.T. McKee, J.Y. Walz, Interaction forces between colloidal particles in a solution of like-charged, adsorbing nanoparticles, J. Coll. Interf. Sci. 365 (2012) 72–80, https://doi.org/10.1016/j.jcis.2011.09.015.
- [25] S. Schön, M. Richter, M. Witt, R. von Klitzing, Externally triggered oscillatory structural forces, Langmuir 34 (2018) 11526–11533, https://doi.org/10.1021/ acs.langmuir.8b02284.
- [26] W.H. Briscoe, Depletion forces between particles immersed in nanofluids, Curr. Opin. Coll. Interf. Sci. 20 (2015) 46–53, https://doi.org/10.1016/ j.cocis.2014.12.002.
- [27] E.D. Goddard, Interactions of surfactants with polymers and proteins, CRC Press, 2018. 10.1201/9781351073783.
- [28] E.D. Goddard, Polymer/surfactant interaction: interfacial aspects, J. Coll. Interf. Sci. 256 (2002) 228–235, https://doi.org/10.1006/jcis.2001.8066.
- [29] E. Guzmán, S. Llamas, A. Maestro, L. Fernández-Peña, A. Akanno, R. Miller, F. Ortega, R.G. Rubio, Polymer-surfactant systems in bulk and at fluid interfaces, Adv. Coll. Interf. Sci. 233 (2016) 38–64, https://doi.org/10.1016/j.cis.2015.11.001.
- [30] R.D. Tilton, In encyclopedia of surface and colloid science, 8th update New York, 2004. 10.1081/E-ESCS-120000637.
- [31] A. Tulpar, R.D. Tilton, J.Y. Walz, Synergistic effects of polymers and surfactants on depletion forces, Langmuir 23 (2007) 4351–4357, https://doi.org/10.1021/ la063191d.
- [32] S. Ji, J.Y. Walz, Synergistic effects of nanoparticles and polymers on depletion and structural interactions, Langmuir 29 (2013) 15159–15167, https://doi.org/ 10.1021/la403473g.
- [33] J.Y. Walz, A. Sharma, Effect of long range interactions on the depletion force between colloidal particles, J. Coll. Interf. Sci. 168 (1994) 485–496, https://doi. org/10.1006/jcis.1994.1446.
- [34] W.A. Ducker, T.J. Senden, R.M. Pashley, Direct measurement of colloidal forces using an atomic force microscope, Nature 353 (6341) (1991) 239–241, https://doi.org/10.1038/353239a0.
- [35] C.P. Green, H. Lioe, J.P. Cleveland, R. Proksch, P. Mulvaney, J.E. Sader, Normal and torsional spring constants of atomic force microscope cantilevers, Rev. Sci. Instrum. 75 (2004) 1988–1996, https://doi.org/10.1063/1.1753100.
- [36] A.D. Braem, S. Biggs, D.C. Prieve, R.D. Tilton, Control of persistent nonequilibrium adsorbed polymer layer structure by transient exposure to surfactants, Langmuir. 19 (2003) 2736–2744, https://doi.org/10.1021/ la0265070.
- [37] A. Tulpar, J.Y. Walz, Simultaneous measurement of structural and hydrodynamic forces between colloidal surfaces in complex fluids, Coll. Surf. A Physicochem. Eng. Asp. 300 (2007) 268–280, https://doi.org/10.1016/ j.colsurfa.2007.01.047.
- [38] J. Kim, M.M. Domach, R.D. Tilton, Pyrene micropartitioning and solubilization by sodium dodecyl sulfate complexes with poly(ethylene glycol), J. Phys. Chem. B. 103 (1999) 10582–10590, https://doi.org/10.1021/jp991720z.
- [39] W. Brown, J. Fundin, M. da G. Miguel, Poly(ethylene oxide)-sodium dodecyl sulfate interactions studied using static and dynamic light scattering, Macromolecules 25 (26) (1992) 7192–7198, https://doi.org/ 10.1021/ma00052a019.
- [40] A. Bandyopadhyay, S.P. Moulik, Counterion binding behaviour of micelles of sodium dodecyl sulphate and bile salts in the pure state, in mutually mixed states and mixed with a nonionic surfactant, Coll. Polym. Sci. 266 (1988) 455– 461, https://doi.org/10.1007/BF01457263.

- [41] C. Botre, V.L. Crescenzi, A. Mele, A study on micelle formation in colloidal electrolyte solutions, J. Phys. Chem. 63 (1959) 650–653, https://doi.org/ 10.1021/j150575a004.
- [42] K.N. Mikhelson, Ion-selective electrodes, Springer, Berlin Heidelberg, Berlin Heidelberg, 2013. 10.1007/978-3-642-36886-8.
- [43] R.M. Pashley, B.W. Ninham, Double-layer forces in ionic micellar solutions, J. Phys. Chem. 91 (1987) 2902–2904, https://doi.org/10.1021/j100295a049.
- [44] O.J. Rojas, P.M. Claesson, K.D. Berglund, R.D. Tilton, Coadsorption and surface forces for selective surfaces in contact with aqueous mixtures of oppositely charged surfactants and low charge density polyelectrolytes, Langmuir 20 (2004) 3221–3230, https://doi.org/10.1021/la035752w.
- [45] A. Thibaut, A. Misselyn-Bauduin, J. Grandjean, G. Broze, R. Jérôme, Adsorption of an aqueous mixture of surfactants on silica, Langmuir 16 (2000) 9192–9198, https://doi.org/10.1021/la000302e.
- [46] P. Alexandridis, J.F. Holzwarth, T.A. Hatton, Micellization of poly(ethylene oxide)-poly(propylene oxide)-poly(ethylene oxide) triblock copolymers in aqueous solutions: thermodynamics of copolymer association, Macromolecules 27 (1994) 2414–2425, https://doi.org/10.1021/ma00087a009.
- [47] P.J. Missel, N.A. Mazer, G.B. Benedek, M.C. Carey, Influence of chain length on the sphere-to-rod transition in alkyl sulfate micelles, J. Phys. Chem. 87 (1983) 1264–1277, https://doi.org/10.1021/j100230a032.
- [48] N.J. Chang, E.W. Kaler, The structure of sodium dodecyl sulfate micelles in solutions of water and deuterium oxide, J. Phys. Chem. 89 (1985) 2996–3000, https://doi.org/10.1021/j100260a009.
- [49] G. Marinov, B. Michels, R. Zana, Study of the State of the triblock copolymer poly(ethylene oxide)—poly(propylene oxide)—poly(ethylene oxide) L64 in aqueous solution, Langmuir 14 (2002) 2639–2644, https://doi.org/10.1021/ la971069w.
- [50] S.M. Ghoreishi, Y. Li, D.M. Bloor, J. Warr, E. Wyn-Jones, Electromotive force studies associated with the binding of sodium dodecyl sulfate to a range of nonionic polymers, Langmuir 15 (1999) 4380–4387, https://doi.org/10.1021/ la981313z.
- [51] Y. Kadam, Clouding and hydrodynamic behavior of pluronic-surfactant interaction in aqueous salt solutions, J. Dispers. Sci. Technol. 31 (2010) 870– 876, https://doi.org/10.1080/01932690903223708.
- [52] E. Thormann, On understanding of the Hofmeister effect: how addition of salt alters the stability of temperature responsive polymers in aqueous solutions, RSC Adv. 2 (2012) 8297, https://doi.org/10.1039/c2ra20164j.

- [53] N. Nishikido, Estimation of micellar charge or aggregation number from conductivity and counterion-activity measurements, J. Coll. Interf. Sci. 92 (1983) 588–591, https://doi.org/10.1016/0021-9797(83)90181-9.
- [54] H.C. Evans, 117. Alkyl sulphates. Part I. Critical micelle concentrations of the sodium salts, J. Chem. Soc. (1956) 579, https://doi.org/10.1039/jr9560000579.
- [55] K.C. Tam, E. Wyn-Jones, Insights on polymer surfactant complex structures during the binding of surfactants to polymers as measured by equilibrium and structural techniques, Chem. Soc. Rev. 35 (2006) 693, https://doi.org/10.1039/ b415140m
- [56] J. Seo, J.H. Kim, M. Lee, J. Moon, D.K. Yi, U. Paik, Size-dependent interactions of silica nanoparticles with a flat silica surface, J. Coll. Interf. Sci. 483 (2016) 177– 184, https://doi.org/10.1016/j.jcis.2016.08.041.
- [57] B. Cabane, R. Duplessix, Organization of surfactant micelles adsorbed on a polymer molecule in water: a neutron scattering study, J. Phys. 43 (1982) 1529–1542, https://doi.org/10.1051/jphys:0198200430100152900.
- [58] B. Cabane, R. Duplessix, Decoration of semidilute polymer solutions with surfactant micelles, J. Phys. 48 (1987) 651–662, https://doi.org/10.1051/ jphys:01987004804065100.
- [59] M. Piech, J.Y. Walz, Direct measurement of depletion and structural forces in polydisperse, charged systems, J. Coll. Interf. Sci. 253 (2002) 117–129, https:// doi.org/10.1006/jcis.2002.8503.
- [60] Y. Li, R. Xu, D.M. Bloor, J.F. Holzwarth, E. Wyn-Jones, The binding of sodium dodecyl sulfate to the ABA block copolymer pluronic F127 (EO 97 PO 69 EO 97): an electromotive force Microcalorimetry, and Light Scattering Investigation, Langmuir 16 (2000) 10515–10520, https://doi.org/10.1021/ la000899y.
- [61] J.S. Nambam, J. Philip, Effects of interaction of ionic and nonionic surfactants on self-assembly of PEO-PPO-PEO Triblock copolymer in aqueous solution, J. Phys. Chem. B 116 (2012) 1499-1507, https://doi.org/10.1021/jp208902a.
- [62] J. Jansson, K. Schillén, G. Olofsson, R. Cardoso da Silva, W. Loh, The Interaction between PEO-PPO-PEO triblock copolymers and ionic surfactants in aqueous solution studied using light scattering and calorimetry, J. Phys. Chem. B. 108 (2004) 82–92, https://doi.org/10.1021/jp030792u.
- [63] X. Mi, J. Yuan, Y. Han, H. Liu, H. Liu, X. Gao, C. Xu, J. Zhang, Introduction of anionic surfactants to copolymer micelles: a key to improving utilization efficiency of P123 in synthesis of mesoporous aluminosilicates, Ind. Eng. Chem. Res. 56 (2017) 7224–7228, https://doi.org/10.1021/acs.iecr.7b01142.